



Crustal Contamination of the Mantle-Derived Liuyuan Basalts: Implications for the Permian Evolution of the Southern Central Asian Orogenic Belt

Yuanyang Yu¹, Keqing Zong^{1*}, Yu Yuan¹, Reiner Klemd², Xin-Shui Wang¹, Jingliang Guo¹,
Rong Xu³, Zhaochu Hu¹, Yongsheng Liu¹

1. State Key Laboratory of Geological Processes and Mineral Resources, School of Earth Sciences,
China University of Geosciences, Wuhan 430074, China

2. GeoZentrum Nordbayern, Universität Erlangen-Nürnberg, Schlossgarten 5a, Erlangen D-91054, Germany

3. State Key Laboratory of Ore Deposit Geochemistry, Institute of Geochemistry, Chinese Academy of Sciences, Guiyang 550081, China

 Yuanyang Yu: <https://orcid.org/0000-0002-3900-0644>;  Keqing Zong: <https://orcid.org/0000-0002-7106-0348>

ABSTRACT: The Permian basalts in the Central Asian Orogenic Belt (CAOB) are crucial for constraining the closure of the Paleo-Asian Ocean. However, the origin of these basalts is still under discussion. Here, we present comprehensive bulk-rock geochemical, Sr-Nd-Pb-Hf isotopic, and zircon U-Pb-Lu-Hf isotopic data of the Liuyuan basalts and coexisting gabbros, which are located in the Beishan Orogen in the southern CAOB, to constrain their emplacement setting and tectonic implications. Our new gabbro ages of ca. 288–294 Ma are interpreted to represent the formation time of the Liuyuan basaltic belt. The Liuyuan basalts show MORB-like rare earth element (REE) patterns and bulk-rock $\varepsilon_{\text{Hf}}(t)$ and $\varepsilon_{\text{Nd}}(t)$ values of 11.0–15.4 and 4.6–9.2, respectively, suggesting an origination mainly from a depleted mantle source. However, positive Pb anomalies, Nb-Ta depletions, and high Th/Yb ratios as well as evolved Sr-Nd-Pb-Hf isotopic compositions of some samples indicate variable continental crustal contribution. According to the covariation of Pb anomalies ($\text{Pb}^* = 2 \times \text{Pb}_N / (\text{Ce}_N + \text{Pr}_N)$) with Sr-Nd-Pb-Hf isotopic compositions, we speculate that parent magma of the Liuyuan basalt was contaminated by continental crustal materials during the eruption rather than having been generated from an enriched mantle source. As revealed by mixing modelling, the Liuyuan basaltic magmas would require a minor (<10%) upper continental crustal assimilation to explain the enriched trace elemental and radiogenic Sr-Nd-Pb-Hf isotopic signatures. Consequently, the Liuyuan basaltic belt is believed to have been generated in a continental extensional environment instead of an oceanic setting and does not constitute a Permian ophiolitic suture zone as previously suggested, since the Paleo-Asian Ocean was already closed in the southern Beishan Orogen in the Early Permian.

KEY WORDS: crustal contamination, Liuyuan basaltic belt, Central Asian Orogenic Belt, Beishan Orogen, Pb anomaly, tectonics.

0 INTRODUCTION

Mantle-derived basalts, which are widely distributed in oceanic and continental plates, play an important role in understanding mantle processes (Hofmann, 2007; Donnelly et al., 2004; Zindler and Hart, 1986; Allègre et al., 1982; White and Hofmann, 1982), crust formation (O'Hara and Herzberg, 2002), and crust-mantle interaction (Jackson et al., 2007; Workman et al., 2004; McBride et al., 2001; Chesley and Ruiz,

1998; Reiners et al., 1995). Based on the enriched geochemical signatures, the mantle sources of oceanic basalts were divided into several end-members such as HIMU, EM1, and EM2 due to variable crustal-mantle recycling (White, 2015; Hofmann, 2007, 1997; Zindler and Hart, 1986). Continental basalts, however, have to transect thick continental lithosphere during ascent, which favors assimilation of continental crustal materials to enrich basaltic magmas. Therefore, although some researchers suggest that the evolved Sr-Nd-Pb-Hf isotopic signatures of continental basalts are derived from an enriched mantle source (e.g., Hofmann, 2007; Farmer, 2003; Zindler and Hart, 1986; Allègre et al., 1982), others argue that crustal contamination plays an important role in the geochemical diversity of these basalts (e.g., Heinonen et al., 2022; Jung et al., 2011; Zeng et al., 2011; Glazner and Farmer, 1992).

Basalts commonly distribute in orogenic belts and bear

*Corresponding author: kqzong@hotmail.com

© China University of Geosciences (Wuhan) and Springer-Verlag GmbH Germany, Part of Springer Nature 2022

Manuscript received April 9, 2022.

Manuscript accepted June 23, 2022.

significant information to unfold the tectonic evolution history (e.g., Alongkot et al., 2021; Mantle and Collins, 2008; Wang et al., 2007). However, the sources of the enriched components of orogenic basalts are often ambiguous. Generally, geochemical indexes such as Ce/Pb, Nb/U, Zr/Nb, Nb/La as well as Sr-Nd-Pb-Hf isotopes on their own are unable to distinguish enriched components from crustal contamination or subduction-related sediment recycling into the mantle (Lee, 2014; Zeng et al., 2011). Thus, it is imperative to evaluate the potential crustal contamination of orogenic basaltic magmas.

The Central Asian Orogenic Belt (CAOB) is one of the most complex accretionary orogens in the world, which underwent multiple evolution processes including subduction, collision, and the amalgamation of microcontinents, island arcs, seamounts, oceanic plateaus, and the formation of accretionary complexes during the closure of the Paleo-Asian Ocean from the Early Neoproterozoic to the Late Paleozoic (e.g., Cao and Wang, 2021; Cheng et al., 2021; Wang S J et al., 2020; Wang T et al., 2020; Xiao et al., 2018, 2015; Cawood et al., 2009; Kröner, 2007; Windley et al., 2007). The evolution of the southern CAOB and the Paleo-Asian Ocean along the Solonker suture zone has been clearly constrained in the east, while how does it evolves in the west remains under discussion (Li et al., 2022). The Beishan Orogen locates in the southern central margin of the CAOB and is, thus, critical for deciphering the evolution of the southern CAOB and the closely related Paleozoic subduction and closure of the Paleo-Asian Ocean (Chen et al., 2022; Wu et al., 2016; Xiao et al., 2010; Zuo et al., 1991). Furthermore, the southern Beishan Orogen is characterized by an occurrence of the Permian Liuyuan basaltic belt (ca. 1 500 km²), which mainly consists of large-scale pillow lavas and massive gabbros (Fig. 1a; Xiao et al., 2010). Despite several detailed former studies, the tectonic setting of the Liuyuan basaltic belt is still hotly debated, which is dominated by an intracontinental setting (Wang et al., 2017; Xue et al., 2016; Zheng et al., 2014; Su et al., 2013; Zhang et al., 2012a, b; Jiang et al., 2007; Zhou et al., 2004) and a subduction-related setting (Zheng et al., 2020; Mao et al., 2012; Ao et al., 2010; Xiao et al., 2009). The former model implies that the closure of the Paleo-Asian Ocean in the southern Beishan Orogen had occurred in the Silurian or Devonian, as evidenced by the lack of thrust faults, chert, Triassic arc-type units or oceanic sedimentary units (Xu et al., 2019; Wang et al., 2017; Chen et al., 2016; Zhang et al., 2011). In contrast, the latter model defines this belt as an ophiolite complex and shows enriched mantle derived arc-related geochemical characteristics (such as evolved Sr isotopes), suggesting the continuous subduction of the Paleo-Asian Ocean until its final closure at Late Permian to Early Triassic (Zheng et al., 2020; Xiao et al., 2018, 2010; Ao et al., 2012; Mao et al., 2012). However, these enriched geochemical characteristics may come from various geological processes. In addition to the involvement of recycled components by subducted slab, the crustal contamination will also lead to a similar characteristic. Therefore, it should be mentioned that the potential role of crustal contamination has not been considered in detail by the previous studies, preventing a thorough understanding of the generation and corresponding tectonic setting of these mafic rocks.

In this study, we present new bulk-rock elemental, Sr-Nd-Pb-Hf isotopic, and in situ zircon U-Pb-Lu-Hf isotopic compositions of the Liuyuan basalts and gabbros to constrain their petrogenesis. We propose that crustal contamination played a decisive role in generating the Early Permian Liuyuan basalts in an intracontinental setting. Thus, in our opinion, the Liuyuan basaltic belt fails to constitute a Permian ophiolitic suture zone (as suggested by previous studies) and, thus, cannot represent the final closure of the Paleo-Asian Ocean in the southern CAOB.

1 GEOLOGICAL SETTING AND SAMPLES

1.1 Geological Backgrounds

The Beishan Orogen is an essential component of the southern CAOB (Xiao et al., 2010), which is bounded by the Dunhuang block to the south, the Solonker suture belt to the east, and the Eastern Tianshan Orogenic belt to the west. There are Xingxingxia and Altyn Tagh faults on the NW and SE sides, respectively. It comprises several tectonically discrete arc terranes, including the Queershan, Hanshan, Mazongshan, Huaniushan, and Shibanshan terranes, which are separated from each other by the Hongshishan, Shibanjing-Xiaohuangshan, Hongliuhe-Xichangjing, and Liuyuan ophiolitic mélanges from the north to the south (Fig. 1a). The Beishan Orogen was divided into two parts by the Early Paleozoic Hongliuhe-Xichangjing ophiolite belt in the central (Song et al., 2015). The northern Beishan Orogen (NBO) is characterized by Paleozoic magmatic arcs, reflecting a complicated collage accretionary system (Cleven et al., 2015; Song et al., 2013; Ao et al., 2012; Xiao et al., 2010), while the southern Beishan Orogen (SBO) is typified by Neoproterozoic (930–900 Ma) and Mesoproterozoic (ca. 1.4 Ga) granitic gneiss, representing a convergence process between microcontinents (Yuan et al., 2019, 2015; He et al., 2014a).

The Liuyuan basaltic belt located in the southern margin of the Beishan Orogen, which was regarded as the constituent of the Liuyuan ophiolitic mélange and possibly represents the southern boundary of the CAOB (Xiao et al., 2010). It covers 150 km long and 10 km wide and separates the Huaniushan terrane from the Shibanshan terrane (Fig. 1a). On the south and north sides of the Liuyuan basaltic belt, Permian volcanic rocks and associated volcanoclastic sedimentary units (e.g., volcanic-bearing sandstones, conglomerates, coarse to fine grained sandstones, claystones, and black shales) covered various Ordovician–Silurian metamorphic rocks and magmatic rocks (Fig. 1b). The Permian sedimentary sequences on both sides of this belt are comparable and symmetrical in petrology and age, which is reconciled with the syncline structure developed in this area (Wang et al., 2017; Jiang et al., 2007). The Permian claystones show contact metamorphism by Liuyuan basalt, suggesting that the Liuyuan basalt was formed later than the Permian claystones (Wang et al., 2017). The Liuyuan basaltic belt is mainly composed of basaltic pillow lavas with minor gabbros, andesites, dacites, rhyolites, and lacustrine sedimentary rocks (sandstone, claystone, and clayey lake deposits; Jiang et al., 2007). Mafic-ultramafic intrusive rocks exposed on the northwest side of the Liuyuan basaltic belt in a NE-SW orientation, almost parallel to the belt's strike. Sedimentary

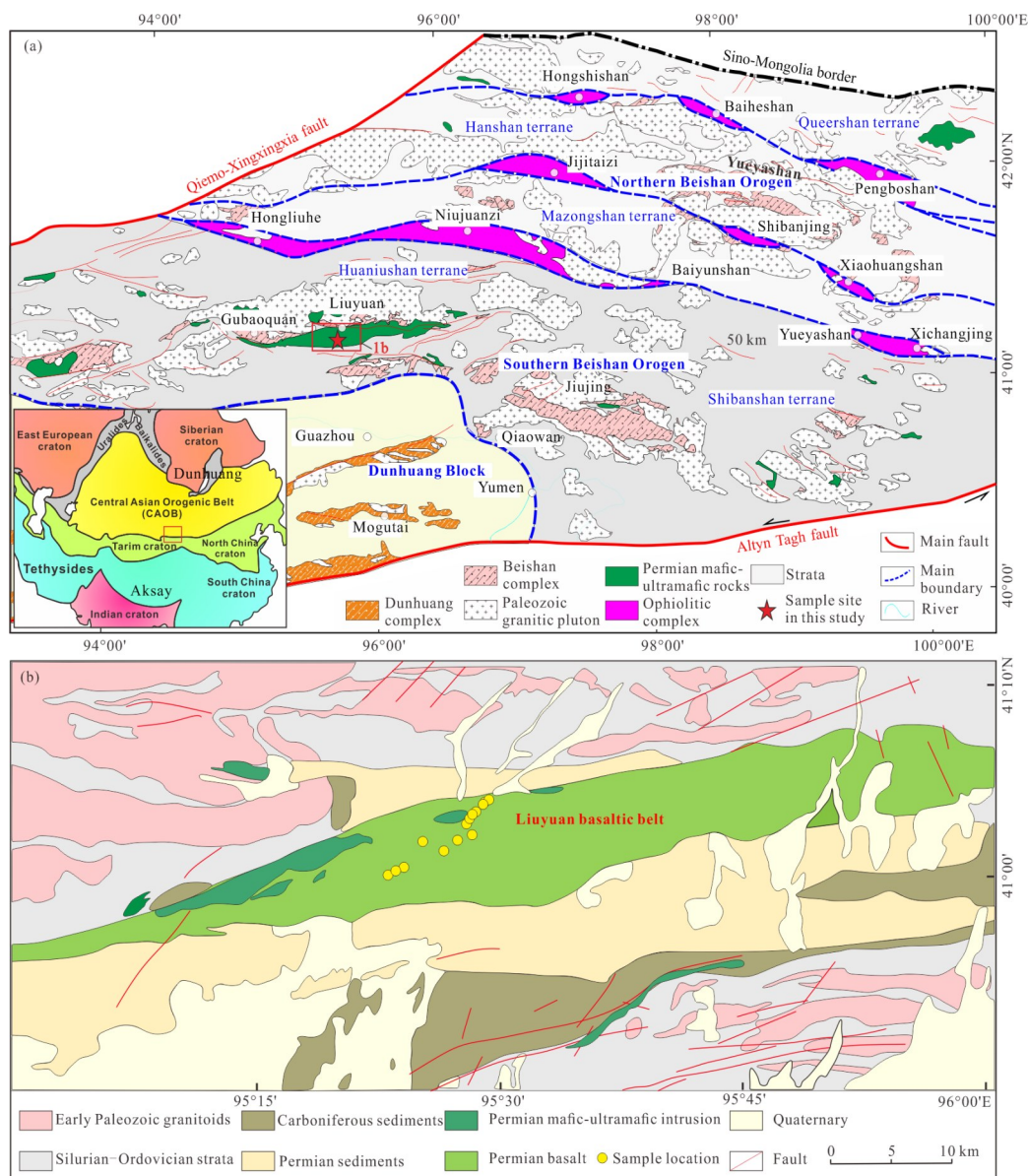


Figure 1. (a) Simplified tectonic map of the Beishan Orogen showing the tectonic subdivisions and studied regions (modified after Xiao et al. (2010) and (He et al., 2015)). Insert figure shows a simplified tectonic map of the Central Asian Orogenic Belt (CAOB) (modified after Xiao et al. (2010)). (b) Geological map of the Liuyuan basaltic belt in the southern Beishan Orogen.

rocks, dacites and rhyolites interlayered with pillow basalts yield zircon U-Pb ages of 277–291 Ma, meaning that basalts were formed contemporaneously with these rocks (Wang et al., 2017). The gabbros intruded into the pillow lavas and sedimentary rocks reveal emplacement ages of 270–282 Ma (Wang et al., 2017). They share identical geochemical signatures with the basaltic pillow lavas implying a comagmatic origin (Wang et al., 2017; Zhang et al., 2011).

1.2 Petrography of Samples

We collected 12 basalt and 2 gabbro samples in the center of the Liuyuan basaltic belt. The sample collection section crosses this belt in a NE-SW direction. The Liuyuan basalts with 0.5–1 m pillow structure in diameter are dark to grey-green (Fig. 2a) and show cryptocrystalline and microcrystalline textures. These rocks are mainly composed of fine-grained to

microlitic plagioclase and clinopyroxene with subordinate Fe-Ti oxides (Fig. 2c). The gabbros have an intrusive contact relationship with the basalts. The (dark)-grey massive gabbros display medium-fine grained and gabbroic texture (Figs. 2b, 2d), typically consisting of platy labradoritic plagioclase (40 vol.%–50 vol.%) and short prismatic clinopyroxene (50 vol.%–60 vol.%) (Fig. 2d). There are also a few amounts of opaque Fe-Ti oxides.

2 ANALYTICAL METHODS

2.1 Whole-Rock Major and Trace Element Analysis

The collected samples were crushed to less than 60 mesh in a corundum jaw crusher. About 100 g was powdered in a vibratory disc mill (RS200, Retsch GmbH, Germany) equipped with a tungsten carbide milling cup to 200 mesh. The bulk-rock major element compositions were measured by X-ray flu-



Figure 2. (a), (b) Field occurrences of the typical rocks in the Liuyuan basaltic belt, including pillow basalts (a) and massive gabbros (b). (c), (d) The respective mineral assemblages of the Liuyuan basalts (c) and gabbros (d). Cpx, clinopyroxene; Pl, plagioclase.

orescence (XRF) using fused glass disks at the State Key Laboratory of Geological Processes and Mineral Resources, China University of Geosciences, Wuhan. The detailed sample-digesting procedure for XRF analyses is the same as in Ma et al. (2012). The analytical precision and accuracy for major element compositions are listed in Table S1.

About 50 mg of sample rock powder was digested by HF + HNO₃ in Teflon bombs and analyzed for trace elements by inductively coupled plasma mass spectrometry (Agilent 7500a ICP-MS) at the State Key Laboratory of Geological Processes and Mineral Resources, China University of Geosciences, Wuhan. The detailed sample-digesting procedure was reported by Liu et al. (2008b). The results of the analyses of standard materials (BHVO-2, AGV-2, and BCR-2) and blanks are summarized in Table S2.

2.2 Zircon U-Pb Dating and Trace Element Analysis by LA-ICP-MS

Zircon grains were separated and concentrated from ~5 kg of crushed gabbros using standard gravimetric and magnetic techniques. U-Pb dating and trace element analysis of zircon grains were performed simultaneously by LA-ICP-MS at the State Key Laboratory of Geological Processes and Mineral Resources, China University of Geosciences, Wuhan. The operating conditions for the laser ablation system and the ICP-MS instrument and data reduction are given in previous studies (Liu et al., 2010, 2008a). The Geolas 2005 excimer ArF laser ablation system was selected as a laser sampling system (Lambda Physik, Göttingen, Germany). An Agilent 7500a ICP-MS instrument was used to acquire ion-signal intensities. A “wire” signal smoothing device was included in this laser ablation sys-

tem (Hu et al., 2012a). Helium was used as a carrier gas and argon as a make-up gas and mixed with the carrier gas via a T-connector before entering the ICP. Each analysis incorporated a background acquisition of approximately 20–30 s (gas blank) followed by a 50 s data acquisition from the sample. Zircon 91500 and NIST610 were used as external standards for U-Pb dating and trace element analysis correction, respectively. Off-line selection and integration of background and analyzed signals, time-drift correction and quantitative calibration for trace element analysis and U-Pb dating were performed by ICPMS-DataCal (Liu et al., 2008a, b). Concordia diagrams and weighted mean calculations were made using Isoplot/Ex_ver3 (Ludwig, 2003). Common-Pb corrections were made using the method of Andersen (2002).

2.3 *In situ* Lu-Hf Isotope Analysis of Zircon by LA-MC-ICP-MS

In situ Lu-Hf isotopic analyses were conducted using a Neptune Plus MC-ICP-MS (Thermo Fisher Scientific, Germany) equipped with a Geolas 2005 excimer ArF laser ablation system (Lambda Physik, Göttingen, Germany) at the State Key Laboratory of Geological Processes and Mineral Resources, China University of Geosciences, Wuhan. A “wire” signal smoothing device was also included in this laser ablation system (Hu et al., 2012a). A simple Y junction was used downstream from the sample cell to add small amounts of nitrogen (4 mL/min) to the argon make-up gas flow (Hu et al., 2008). In the present study, all zircon data were acquired in single spot ablation mode at a spot size of 44 µm. Each measurement consisted of 20 s of acquisition of the background signal followed by 50 s of ablation signal acquisition. Detailed operating condi-

tions for the laser ablation system, the MC-ICP-MS instrument, and the analytical methods are given in Hu et al. (2012b). ICPMSDataCal was used to solve off-line selection and integration of the analyte signals, and mass bias calibrations (Liu et al., 2010, 2008a)

2.4 Whole-Rock Sr-Nd-Pb-Hf Isotopic Analyses

The Sr-Nd-Pb-Hf isotopic analyses, including sample dissolution, column chemistry, and measurement, were performed at the Wuhan SampleSolution Analytical Technology Co., Ltd., Hubei, China. Based on Sr-Nd-Pb-Hf concentrations, about 50–200 mg of sample powder (200 mesh) was digested in mixed HNO₃ and HF solution in Teflon bombs. Then the Teflon bombs were heated to 190 °C for >24 h in a stainless steel pressure jacket. After cooling, the solution was dried on a hotplate at 140 °C, and then 1 mL HNO₃ was added and evaporated to dryness again. Lastly, the sample was dissolved in the different acid solutions for column chemistry. For Sr isotopic separation, the samples were separated on ion-exchange columns by AG50W resin. The Nd isotopes were eluted in the evaporated REE solution by an ion-exchange column filled with LN resin. The AG resin was used to separate Pb isotopes, and the Hf isotopes were separated by LN-Spec resin.

The Sr-Nd-Pb-Hf isotopic analyses were performed on a Neptune Plus MC-ICP-MS (Thermo Fisher Scientific, Dreieich, Germany). Aliquots of the international standard solutions of NIST SRM 987, JNDI-1, and JMC 475 were regularly used for evaluating the reproducibility and accuracy of the instrument for Sr-Nd-Pb-Hf isotopes. All data reduction for the MC-

ICP-MS analyses of the Sr-Nd-Pb-Hf isotopic ratios was conducted using the “Iso-Compass” software (Zhang et al., 2020). The USGS reference material BCR-2 (basalt) was used to monitor the data quality and its ⁸⁷Sr/⁸⁶Sr (0.705 046 ± 0.000 012), ¹⁴³Nd/¹⁴⁴Nd (0.512 650 ± 0.000 007), ¹⁷⁶Hf/¹⁷⁷Hf (0.282 870 ± 0.000 006), ²⁰⁸Pb/²⁰⁴Pb (38.716 ± 0.003), ²⁰⁷Pb/²⁰⁴Pb (15.625 ± 0.001), and ²⁰⁶Pb/²⁰⁴Pb (18.748 ± 0.001) ratios, all of which were consistent with recommended values within errors (Table S3, Zhang and Hu, 2020).

3 RESULTS

3.1 Zircon U-Pb Ages and Lu-Hf Isotopic Compositions

Zircon U-Pb ages and Lu-Hf isotopic compositions are listed in Tables S4–S5. The zircon grains separated from the gabbro samples (13LY42 and 13LY43) range in length from 80 to 200 μm and have length-to-width ratios between 1 : 1 and 2 : 1. The zircon grains are colorless and transparent or semi-transparent. Most zircon grains are euhedral or subhedral and show weak oscillatory or homogeneous zoning as revealed by the cathodoluminescence (CL) images (Figs. 3c, 3d). Their Th/U ratios range from 0.7 to 3.1. The zircon grains of two samples yield concordant or near concordant U-Pb ages with weighted mean ²⁰⁶Pb/²³⁸U ages of 288 ± 1 Ma (2σ; n = 21, MSWD = 1.7, sample 13LY42) and 294 ± 1 Ma (2σ; n = 22, MSWD = 1.5, sample 13LY43), respectively (Figs. 3a, 3b).

Samples 13LY42 and 13LY43 show initial zircon ¹⁷⁶Hf/¹⁷⁷Hf ratios of 0.282 98–0.283 08 and 0.282 96–0.283 01, and ε_{Hf}(t) values from +14 to +17 and +13 to +15, respectively (Table S5).

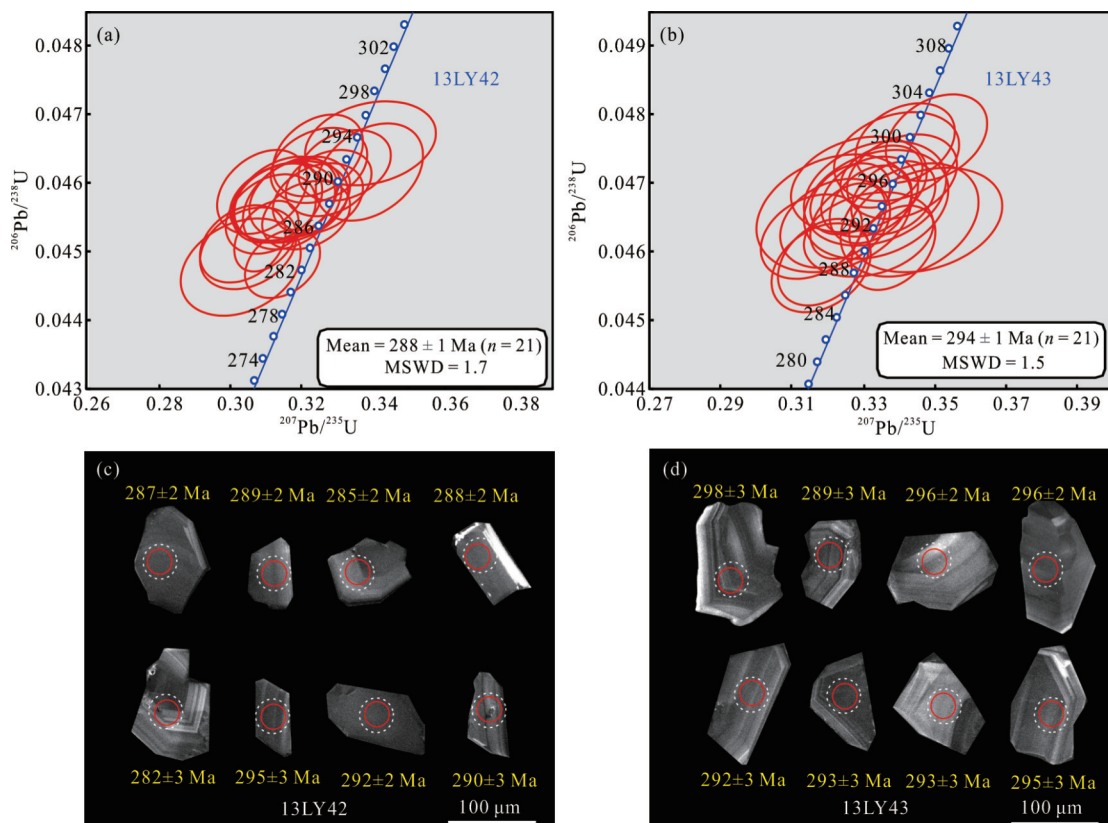


Figure 3. Zircon U-Pb Concordia diagrams (a), (b) and cathodoluminescence (CL) images (c), (d) of two gabbros (samples 13LY42 and 13LY43) from the Liuyuan basaltic belt.

3.2 Bulk-Rock Elemental Compositions

The Liuyuan basalts and gabbros mainly belong to the sub-alkaline series on the TAS diagram (Fig. 4, all values in text and figures recalculated on a normalized anhydrous basis). Both basalts and gabbros have relatively low LOI ratios (1.51–3.03) (Table S6). The basalts exhibit a relatively narrow range of SiO₂ (46.6 wt.%–52.0 wt.%), TiO₂ (0.6 wt.%–2.9 wt.%), FeO_T (10.0 wt.%–13.9 wt.%), MgO (4.3 wt.%–9.3 wt.%), CaO (7.2 wt.%–11.8 wt.%) and Al₂O₃ (12.9 wt.%–15.1 wt.%) contents, respectively (Table S6, Fig. 5). Comparatively, the TiO₂ and FeO_T contents of the gabbros are slightly lower than those of the basalts (Table S6, Figs. 5c, 5d).

All samples show N-MORB-like flat rare earth element (REE) patterns ($(La/Yb)_N = 0.75–1.96$) with weak negative Eu anomalies ($Eu^* = 0.79–1.06$; Figs. 5f, 6a) on the chondrite-normalized REE diagram, while the REE contents of the basalts are usually higher than those of the gabbros (Fig. 6a). On the primitive mantle-normalized trace element diagram, the Liuyuan basalts and gabbros show negative Nb, Ta, Ti, and strongly variable Pb anomalies (Fig. 6b). These trace element characteristics are consistent with those of previously studied Permian basalts and gabbros in this area (Mao et al., 2012; Zhang et al., 2011; Jiang et al., 2007) (grey shadow in Fig. 6).

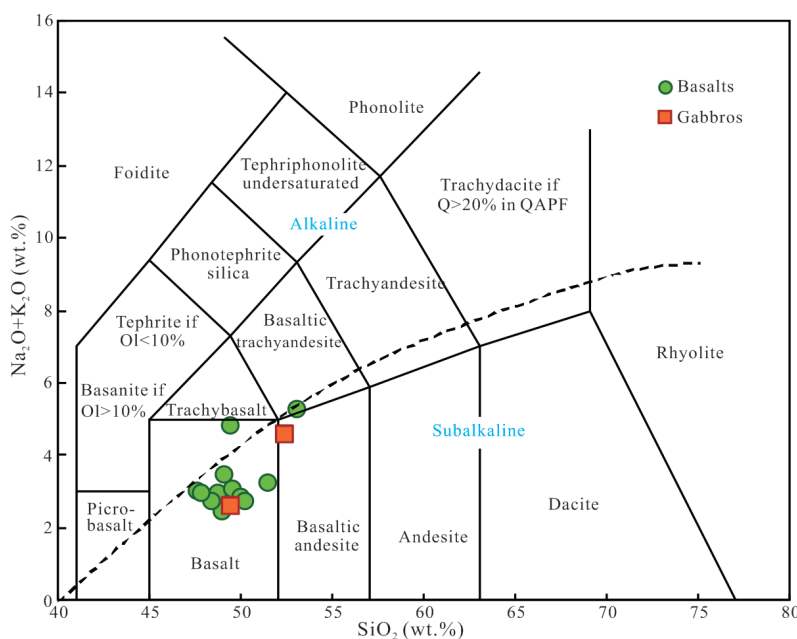


Figure 4. The SiO₂ versus total alkali (Na₂O+K₂O) diagram for the Liuyuan basalts and gabbros. Rock type boundaries are from Bas et al. (1986).

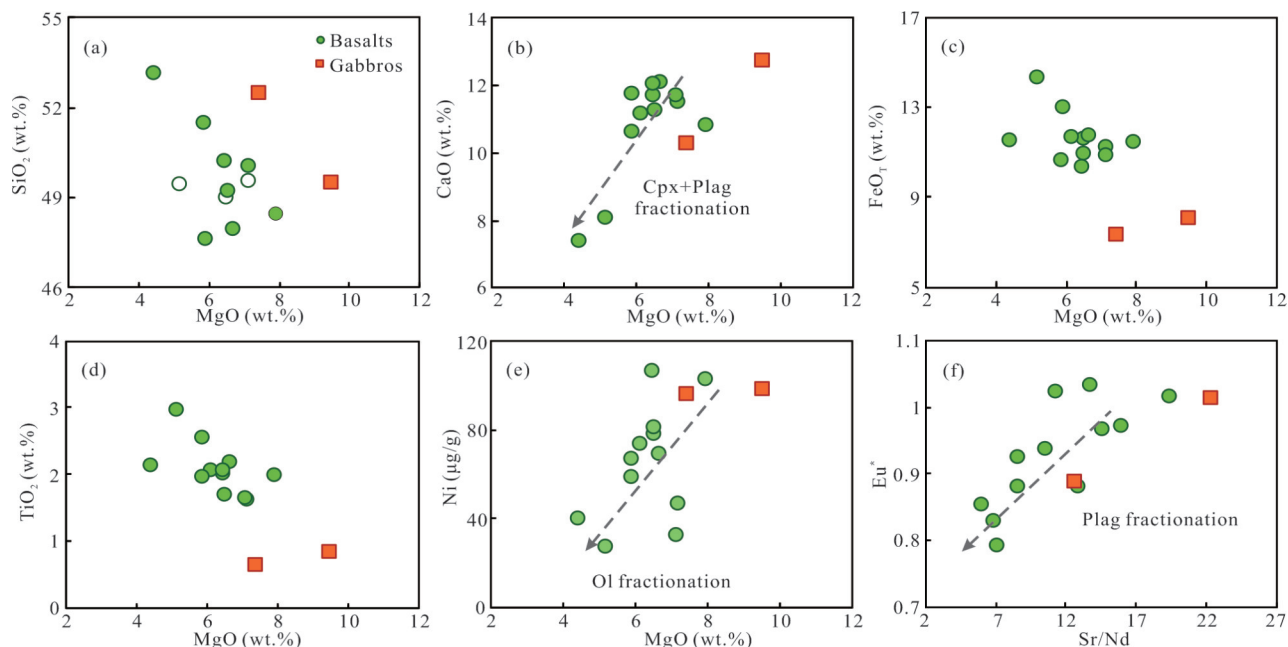


Figure 5. (a)–(e) Covariations of MgO with SiO₂, CaO, FeO_T, TiO₂, and Ni and (f) $Eu^* (2 \times Eu_N / (Sm_N + Gd_N))$ vs. Sr/Nd for the Liuyuan basalts and gabbros. Cpx. Clinopyroxene; Plag. plagioclase.

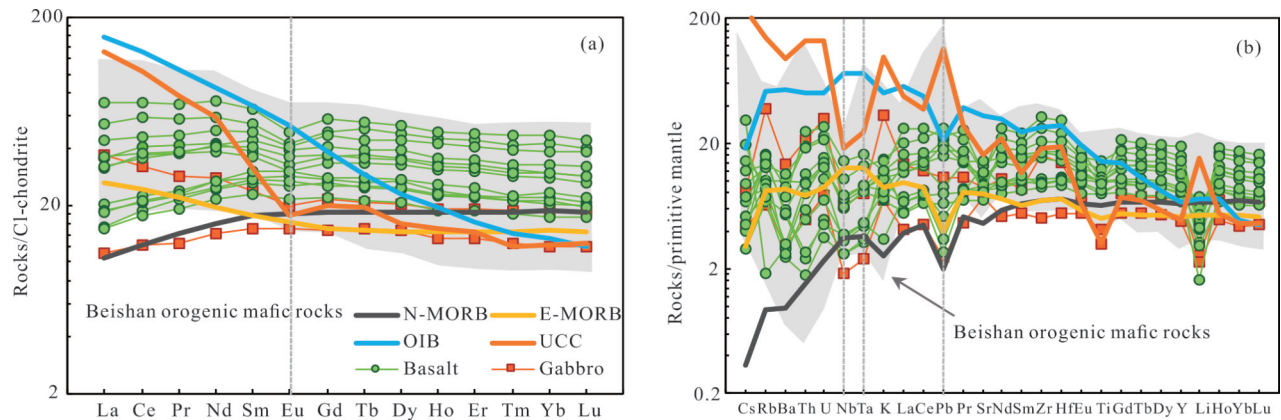


Figure 6. (a) CI-chondrite normalized REE patterns and (b) primitive mantle normalized spider diagrams of the Liuyuan basalts and gabbros in the southern Beishan Orogen. The CI-chondrite and primitive mantle values are from McDonough and Sun (1995). The shaded areas show the data from the references (Zheng et al., 2020, 2014; Xu et al., 2019; Zhang et al., 2015, 2011; Su et al., 2012; Zhao et al., 2006). N-MORB and E-MORB are from Gale et al. (2013), OIB is from GEOROCK (<http://georoc.mpch-mainz.gwdg.de/georoc/>), and UCC is from Rudnick and Gao (2003).

3.3 Sr-Nd-Pb-Hf Isotope Compositions

The Liuyuan basalts and gabbros show a large range of Sr-Nd-Pb-Hf isotopic compositions (Fig. 7). Their initial $^{87}\text{Sr}/^{86}\text{Sr}_{\text{initial}}$ ratios, $\epsilon_{\text{Nd}}(t)$, and $\epsilon_{\text{Hf}}(t)$ values are $0.703\,01\text{--}0.705\,49$, $+4.6\text{--}+9.2$, and $+11.0\text{--}+15.5$, respectively (Table S7). Their $^{206}\text{Pb}/^{204}\text{Pb}_{\text{initial}}$, $^{207}\text{Pb}/^{204}\text{Pb}_{\text{initial}}$, and $^{208}\text{Pb}/^{204}\text{Pb}_{\text{initial}}$ ratios are $17.80\text{--}18.36$, $15.53\text{--}15.58$, and $37.69\text{--}38.24$, respectively (Table S7).

4 DISCUSSION

4.1 Fractional Crystallization of the Liuyuan Basalts

Petrographic and geochemical observations indicate that the Liuyuan basalts experienced fractional crystallization with the formation of olivine, plagioclase, and pyroxene, as well as previous reports (Wang et al., 2016; Mao et al., 2011; Zhang et al., 2011; Jiang et al., 2007; Zhao et al., 2006). The obvious positive relationship between Ni and MgO indicates substantial fractional crystallization of olivine (Fig. 5e). The slightly negative Eu anomaly (Fig. 6a) and the correlation between Sr/Nd and Eu^* , indicate the crystallization of plagioclase. While the range of CaO (7.2 wt.%–12.5 wt.%) and Al_2O_3 (12.9 wt.%–15.8 wt.%) highlights the variability produced by plagioclase and/or clinopyroxene fractionation (Fig. 5b). However, fractional crystallization usually does not result in highly variable Pb anomalies and a wide range of Sr-Nd-Pb-Hf isotope compositions. These characteristics all indicate that the Liuyuan basalts may be subjected to the addition of crustal components, and the relevant process will be discussed in the next section.

4.2 Crustal Contamination and the Origin of the Liuyuan Basalts

The gabbro samples are excluded from bulk-rock trace element fingerprinting due to variable degrees of fractional crystallization (Pearce, 2003). In contrast, the whole-rock geochemistry of basalts generally represents original magma compositions, which are less affected by crystallization processes, especially the highly incompatible element patterns (e. g., Nb, Ta, Ti) and radioisotope compositions (e. g., Sr, Nd, and Hf isotopes). The Liuyuan basalts show Nb-Ta-Ti depletions and strongly variable Pb anomalies (Fig. 6b), indicating the addi-

tion of an enriched component. Only a few of the Liuyuan basalts exhibit high Ce/Pb ratios (>20) that are close to MORB (Ce/Pb = 25 ± 5 ; (Hofmann et al., 1986), while the majority of samples show distinctly lower Ce/Pb ratios (<12) that are typical signatures of continental crust (Gao et al., 1998; Rudnick and Fountain, 1995). The evolved Sr-Nd-Pb-Hf isotopic compositions (Fig. 7) also indicate the addition of the Liuyuan mafic magmas by enriched materials such as continental crust or sediments. However, it is usually difficult to pinpoint the exact timing and location of the addition of these enriched materials, i. e., contamination of the crustal sediments in the mantle source region or assimilation during the ascent and extrusion of the magmas after departure from the mantle source.

Mao et al. (2011) suggested that the high and varied $^{87}\text{Sr}/^{86}\text{Sr}$ ratios (0.703 4–0.709 8) of the Liuyuan basalts are the result of slab-derived components mixing in the mantle source. However, the here reported $\epsilon_{\text{Hf}}(t) = +15.4$ and $\epsilon_{\text{Nd}}(t) = +9.2$ values of the Liuyuan basalts are similar to those of the depleted mantle (Zindler and Hart, 1986). Furthermore, the Liuyuan basalts show strongly variable Pb anomalies relative to MORB and OIB and, in addition, exhibit excellent Pb^* ($2 \times \text{Pb}_N / (\text{Ce}_N + \text{Pr}_N)$) and Sr-Nd-Pb-Hf isotope correlations (Fig. 7), which are not shown by the most OIB that are considered to have an enriched mantle source (White, 2010). Although the samples were slightly altered (LOI = 1.51–3.03), there is no correlation with Pb^* , which excludes the possible influence of secondary processes such as late hydrothermal alteration on Pb^* (Fig. S1). Therefore, crustal contamination of the Liuyuan mafic magmas after their departure from the mantle source region should play an important role in the generation of the enriched isotope signatures of the basalt. Moreover, the crustal contamination becomes more powerful with the evolution of the magma, as evidenced by the good correlations between MgO and Pb^* , $^{208}\text{Pb}/^{204}\text{Pb}_{\text{initial}}$, $^{87}\text{Sr}/^{86}\text{Sr}_{\text{initial}}$ and Ce/Pb (Fig. 8). It can be further demonstrated that Pb^* is an effective index of crustal contamination. Besides, the occurrence of the crustal contamination of the Liuyuan mafic magmas is also supported by the gabbro sample 13LY42 which has a lower bulk-rock $\epsilon_{\text{Hf}}(t)$ value ($+13$) than the early-crystallized zircons ($\epsilon_{\text{Hf}}(t) = +14\text{--}+17$) (Fig.

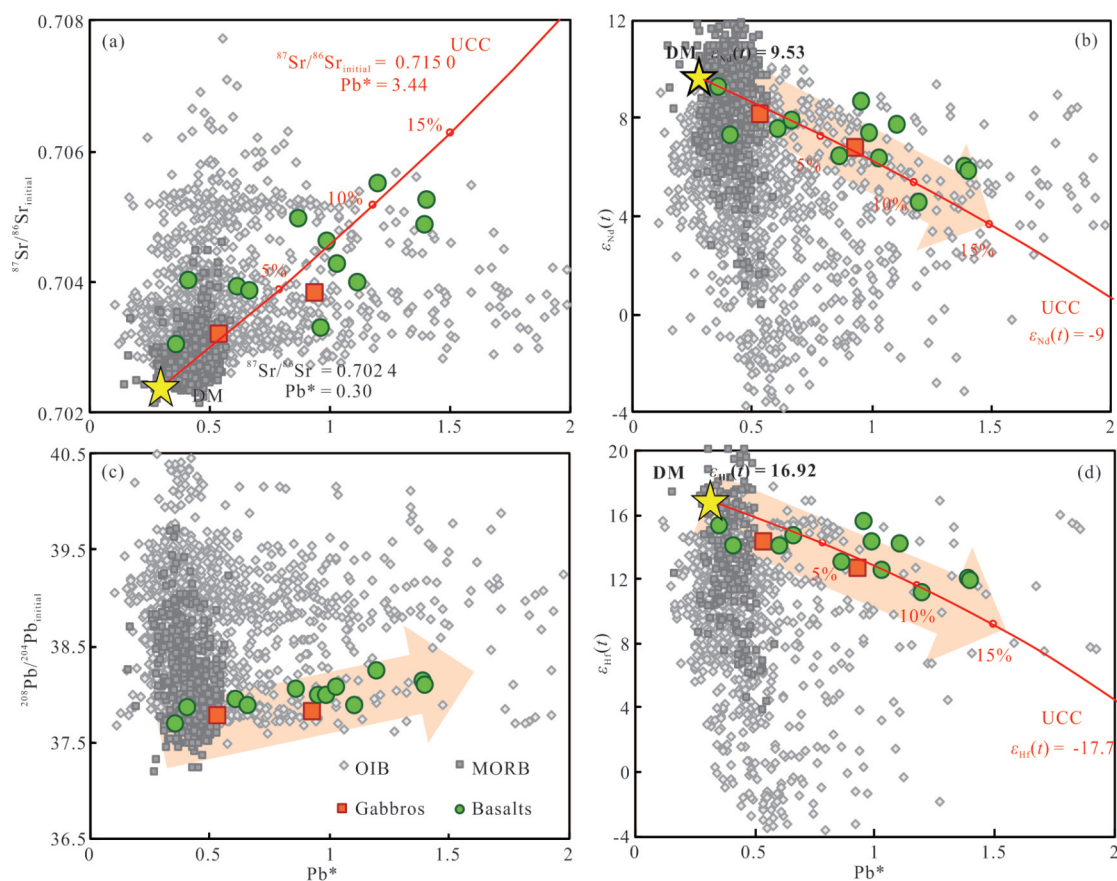


Figure 7. Covariations of Pb^* ($2 \times Pb_N / (Ce_N + Pr_N)$) with initial $^{87}Sr/^{86}Sr_{initial}$ (a), $\epsilon_{Nd}(t)$ (b), $^{208}Pb/^{204}Pb_{initial}$ (c) and $\epsilon_{Hf}(t)$ (d) of the Liuyuan basalts and gabbros in the southern Beishan Orogen. The $^{87}Sr/^{86}Sr_{initial}$, $\epsilon_{Nd}(t)$, and $\epsilon_{Hf}(t)$ of upper continental crust (UCC) and depleted mantle (DM) are from Jahn et al. (2000) and Workman and Hart (2005), respectively. The Pb^* of UCC and the DM-derived MORB are calculated from Gale et al. (2013); Rudnick and Gao (2003). Gray squares and the light gray diamonds represent MORB (Gale et al., 2013) and OIB (GEOROCK (<http://georoc.mpch-mainz.gwdg.de/georoc/>)), respectively.

9), thereby indicating that substantial crustal contamination of the basaltic magmas had occurred and contributed to lots of the whole rock Hf isotopic composition and within zircons preserved the early signature of depletion.

In summary, the Liuyuan basalts and the associated gabbros, which were derived from the same depleted mantle source, underwent significant crustal contamination. In order to identify that the enriched materials mainly come from the upper crust or the lower crust and evaluate the proportion of the contamination, we conducted mixing modelling between depleted mantle (DM) and the upper continental crust (UCC) or the lower continental crust (LCC) using Th/Yb, Nb/Yb ratios, which represent the interaction between continental crust and magmas (Pearce and Peate, 1995). High Th/Yb ratios deviated from the MORB-OIB array (Fig. 9), which indicates the involvement of crustal components (Pearce, 2008). In the Th/Yb-Nb/Yb diagram, the Liuyuan basalts more likely experienced about 10% contamination of the UCC rather than the LCC. Because >50% contamination of LCC is impossible (Fig. 10a). The mixing modelling of Pb^* vs. $^{87}Sr/^{86}Sr_{initial}$, $\epsilon_{Nd}(t)$, and $\epsilon_{Hf}(t)$ between DM and UCC further suggests that about 10% contamination of UCC is reasonable (Fig. 7). Moreover, the modelling simulation of Sr-Nd isotopic compositions of DM with UCC also shows that the Liuyuan basalts were contaminated by UCC with a proportion of about 10% (Fig. 10b).

4.3 Implication for the Final Closure of the Paleo-Asian Ocean in the Southern CAOB

The Beishan Orogen plays an important role in constraining and understanding the tectonic evolution of the southern CAOB (Zheng et al., 2020; Zhang et al., 2011; Xiao et al., 2010). Xiao et al. (2010) suggested that the Liuyuan basaltic belt is a Permian ophiolitic complex of the Paleo-Asian Ocean in the southern CAOB, which was finally closed in the Triassic based on the supra-subduction zone (SSZ) character of Permian mafic rocks in this area (Zheng et al., 2020; Feng et al., 2018; Mao et al., 2011; Ao et al., 2010; Xiao et al., 2010). However, the lack of marine sediments and the presence of terrigenous clastic rocks do not support this view (Wang et al., 2017; Chen et al., 2016). Moreover, the enriched characteristics (e.g., radiogenic Sr isotope and high LILE contents) found by Mao et al. (2012) in Liuyuan basalts may not be attributed to the contribution of the subduction plate, but rather may be caused by crustal contamination during the ascent and extrusion of magma, as we discussed in Section 4.1. Other studies proposed that the Liuyuan basaltic belt had formed as a result of plume-associated magmatic processes (Su et al., 2012; Qin et al., 2011; Zhou et al., 2004). However, the lack of planar magmatism distribution, a long emplacement time of ~20 Ma, and distinct geochemical features in mantle plume-related mafic rocks refute this hypothesis (Xue et al., 2016; Campbell and Griffiths, 1990).

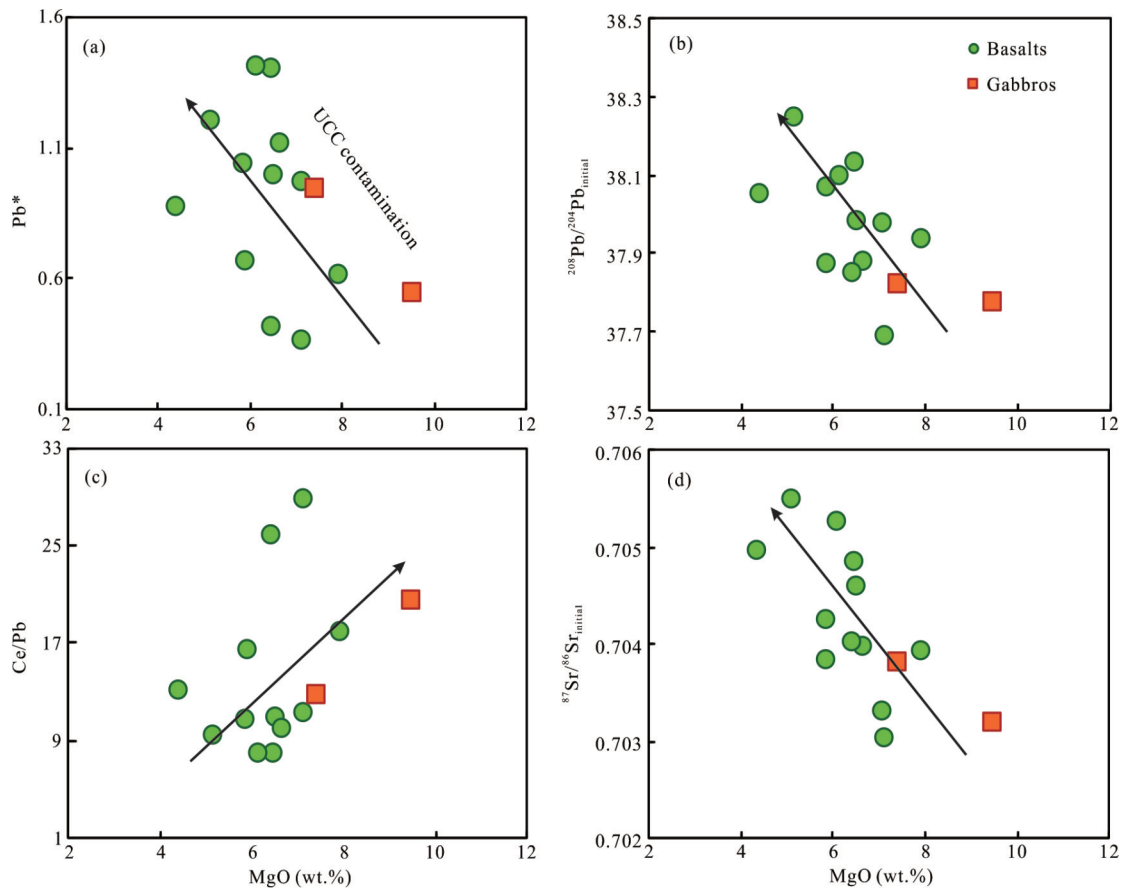


Figure 8. MgO vs. Pb^* ($2 \times Pb_N / (Ce_N + Pr_N)$), $^{208}Pb/^{204}Pb_{initial}$, Ce/Pb, and $^{87}Sr/^{86}Sr_{initial}$ of the Liuyuan basalts and gabbros in the southern Beishan Orogen.

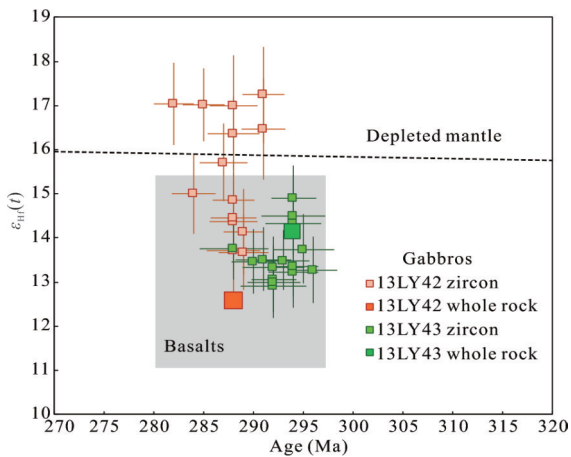


Figure 9. Zircon and whole-rock Hf isotopic compositions of the Liuyuan basalts and gabbros in the southern Beishan Orogen.

Our geochronological results show that the Liuyuan basalt formed in the Early Permian (Figs. 3a, 3b), which is consistent with previous studies (Zhang et al., 2011; Zhao et al., 2006). However, the geochemical characteristics of the Liuyuan basalts unambiguously show that they were contaminated by the upper continental crust (Figs. 7–10). The Late Carboniferous (318–312 Ma) southward subduction in the area 200 km north of this basaltic belt (Zhang et al., 2017) could cause the intracontinental extension environment in the Liuyuan area, which appears to more reasonably explain the mafic rocks, symmetri-

cal, and lacustrine characteristics of the peperite-bearing volcanogenic-sedimentary strata on the north and south sides of the Liuyuan basaltic belt (Wang et al., 2017; Chen et al., 2016). Furthermore, the intracontinental extensional environment can not only explain the widespread occurrence of Permian A-type granite and bimodal volcanic rocks produced under the extensional background in this area (Xu et al., 2018; Wang et al., 2017; Zheng et al., 2014; Zhang et al., 2012b) but also produce pillow basalts with geochemical characteristics of depletion. Therefore, we favor an intracontinental extensional environment, instead of the presence of the Paleo-Asian Ocean in the southern Beishan Orogen during this period. This is also supported by tectonic models such as the intracontinental rift system (Liu et al., 2022; Wang et al., 2017; Jiang et al., 2007) and post-collision delamination settings (Zhang et al., 2011; Zhao et al., 2006). Importantly, the occurrence of ~465 Ma high-pressure (HP) eclogites in the northern of the Liuyuan basaltic belt (Saktura et al., 2017; Liu et al., 2011; Qu et al., 2011) implies an Early Paleozoic subduction and collision event in the southern Beishan Orogen. Moreover, the discovery of ~440–430 Ma HP granulites in the Dunhuang Block indicates that the Dunhuang continental margin has been subducted and collided with the southern Beishan Orogenic belt in the Early Paleozoic (He et al., 2014b; Zong et al., 2012). During the Early Paleozoic, therefore, the terranes in the southern Beishan Orogen have been progressively accreted together in the northern margin of the Dunhuang block and the Paleo-Asian Ocean has been closed in this orogen.

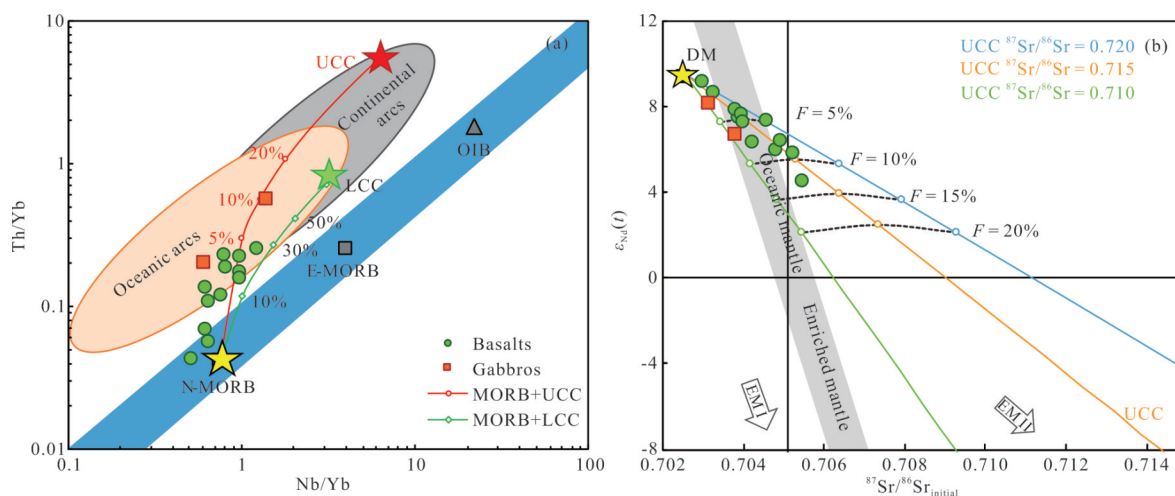


Figure 10. (a) Th/Yb vs. Nb/Yb and (b) whole-rock Sr-Nd isotopic compositions of the Liuyuan basalts and gabbros in the southern Beishan Orogen. Upper continental crust (UCC) and lower continental crust (LCC) values are from Rudnick and Gao (2003). MORB values are from Gale et al. (2013). The end-member of the DM ($\epsilon_{Nd}(t) = 8.70$, $^{87}\text{Sr}/^{86}\text{Sr}_{\text{initial}} = 0.7025$) is from Gale et al. (2013). The end-members of the UCC ($\epsilon_{Nd}(t) = -10$, $^{87}\text{Sr}/^{86}\text{Sr}_{\text{initial}} = 0.710\text{--}0.720$) is from Jahn et al. (2000). The areas of EM1 and EM2 are from Zindler and Hart (1986).

5 CONCLUSIONS

We present comprehensive petrological observation, bulk-rock major and trace elements, Sr-Nd-Pb-Hf isotopic, and zircon U-Pb-Lu-Hf isotopic data of the Liuyuan basalts and gabbros. Zircon grains from two gabbros reveal crystallization ages of 288–294 Ma. The Liuyuan basalts show evolved bulk-rock $^{87}\text{Sr}/^{86}\text{Sr}_{\text{initial}}$ (0.703 103–0.705 49), $^{208}\text{Pb}/^{204}\text{Pb}_{\text{initial}}$ (37.69–38.24) and depleted bulk-rock $\epsilon_{\text{Hf}}(t)$ values (11.0–15.4), $\epsilon_{\text{Nd}}(t)$ values (4.6–9.2) respectively. Based on these geochemical characteristics, we propose that the Early Permian Liuyuan basaltic belt in the southern Beishan Orogen of the southern CAOB derived from a depleted mantle source and experienced about 10% contamination of the upper continental crust. Therefore, the Liuyuan basaltic belt formed in an intracratonic extensional environment and does not constitute an ophiolitic suture zone, thereby indicating that the Paleo-Asian Ocean was already closed in Early Permian in the southern Beishan Orogen of the southern CAOB.

ACKNOWLEDGMENTS

We would like to thank Huai Cheng, Tao Luo, Wen Zhang, and Haihong Chen for their kind support in the lab. This research was co-supported by the National Natural Science Foundation of China (No. 41922021) and the MOST Special Fund from the State Key Laboratory of Geological Processes and Mineral Resources, China University of Geosciences (No. MSFGPMR01-03). The final publication is available at Springer via <https://doi.org/10.1007/s12583-022-1706-1>.

Electronic Supplementary Materials: Supplementary materials (Fig. S1, Tables S1–S7) are available in the online version of this article at <https://doi.org/10.1007/s12583-022-1706-1>.

REFERENCES CITED

Allègre, C. J., Dupré, B., Richard, P., et al., 1982. Subcontinental Versus Suboceanic Mantle. II. NDSRBP Isotopic Comparison of Continental Tholeiites with Mid-Ocean Ridge Tholeiites, and the Structure of the

- Continental Lithosphere. *Earth and Planetary Science Letters*, 57(1): 25–34. [https://doi.org/10.1016/0012-821x\(82\)90170-4](https://doi.org/10.1016/0012-821x(82)90170-4)
- Alongkot, F., Chidchanok, K., Toshiaki, T., et al., 2021. Petrochemistry and Zircon U-Pb Geochronology of Felsic Xenoliths in Late Cenozoic Gem-Related Basalt from Bo Phloi Gem Field, Kanchanaburi, Western Thailand. *Journal of Earth Science*, 32(4): 1035–1052. <https://doi.org/10.1007/s12583-020-1347-1>
- Andersen, T., 2002. Correction of Common Lead in U-Pb Analyses That do not Report ^{204}Pb . *Chemical Geology*, 192(1/2): 59–79. [https://doi.org/10.1016/s0009-2541\(02\)00195-x](https://doi.org/10.1016/s0009-2541(02)00195-x)
- Ao, S. J., Xiao, W. J., Han, C. M., et al., 2012. Cambrian to Early Silurian Ophiolite and Accretionary Processes in the Beishan Collage, NW China: Implications for the Architecture of the Southern Altaids. *Geological Magazine*, 149(4): 606–625. <https://doi.org/10.1017/s0016756811000884>
- Ao, S. J., Xiao, W. J., Han, C. M., et al., 2010. Geochronology and Geochemistry of Early Permian Mafic-Ultramafic Complexes in the Beishan Area, Xinjiang, NW China: Implications for Late Paleozoic Tectonic Evolution of the Southern Altaids. *Gondwana Research*, 18(2/3): 466–478. <https://doi.org/10.1016/j.gr.2010.01.004>
- Bas, M. J. L., Maitre, R. W. L., Streckeisen, A., et al., 1986. A Chemical Classification of Volcanic Rocks Based on the Total Alkali-Silica Diagram. *Journal of Petrology*, 27(3): 745–750. <https://doi.org/10.1093/petrology/27.3.745>
- Cao, S. N., Wang, B., 2021. Age, Origin and Geological Implications of Early Paleozoic Marine Bentonites, Northern Yili Block of Central Asian Orogenic Belt. *Earth Science*, 46(8): 2804–2818 (in Chinese with English Abstract)
- Campbell, I. H., Griffiths, R. W., 1990. Implications of Mantle Plume Structure for the Evolution of Flood Basalts. *Earth and Planetary Science Letters*, 99(1/2): 79–93. [https://doi.org/10.1016/0012-821x\(90\)90072-6](https://doi.org/10.1016/0012-821x(90)90072-6)
- Cawood, P. A., Kröner, A., Collins, W. J., et al., 2009. Accretionary Orogens through Earth History. *Geological Society, London, Special Publications*, 318(1): 1–36. <https://doi.org/10.1144/sp318.1>
- Chen, X. H., Dong, S. W., Shi, W., et al., 2022. Construction of the Continental Asia in Phanerozoic: A Review. *Acta Geologica Sinica-English Edition*, 96(1): 26–51. <https://doi.org/10.1111/1755-6724.14867>

- Chen, S., Guo, Z. J., Qi, J. F., et al., 2016. Early Permian Volcano-Sedimentary Successions, Beishan, NW China: Peperites Demonstrate an Evolving Rift Basin. *Journal of Volcanology and Geothermal Research*, 309: 31–44. <https://doi.org/10.1016/j.jvolgeores.2015.11.004>
- Cheng, Y., Xiao, Q. H., Li, T. D., et al., 2021. An Intra-Oceanic Subduction System Influenced by Ridge Subduction in the Diyanmiao Subduction Accretionary Complex of the Xar Moron Area, Eastern Margin of the Central Asian Orogenic Belt. *Journal of Earth Science*, 32(1): 253–266. <https://doi.org/10.1007/s12583-021-1404-4>
- Chesley, J. T., Ruiz, J., 1998. Crust-Mantle Interaction in Large Igneous Provinces: Implications from the Re-Os Isotope Systematics of the Columbia River Flood Basalts. *Earth and Planetary Science Letters*, 154(1/2/3/4): 1–11. [https://doi.org/10.1016/s0012-821x\(97\)00176-3](https://doi.org/10.1016/s0012-821x(97)00176-3)
- Cleven, N., Lin, S. F., Guilmette, C., et al., 2015. Petrogenesis and Implications for Tectonic Setting of Cambrian Suprasubduction-Zone Ophiolitic Rocks in the Central Beishan Orogenic Collage, Northwest China. *Journal of Asian Earth Sciences*, 113: 369–390. <https://doi.org/10.1016/j.jseas.2014.10.038>
- Donnelly, K. E., Goldstein, S. L., Langmuir, C. H., et al., 2004. Origin of Enriched Ocean Ridge Basalts and Implications for Mantle Dynamics. *Earth and Planetary Science Letters*, 226(3/4): 347–366. <https://doi.org/10.1016/j.epsl.2004.07.019>
- Farmer, G. L., 2003. Continental Basaltic Rocks. *Treatise on Geochemistry*, 3: 659
- Feng, L. M., Lin, S. F., Davis, D. W., et al., 2018. Dunhuang Tectonic Belt in Northwestern China as a Part of the Central Asian Orogenic Belt: Structural and U-Pb Geochronological Evidence. *Tectonophysics*, 747/748: 281–297. <https://doi.org/10.1016/j.tecto.2018.09.008>
- Gale, A., Dalton, C. A., Langmuir, C. H., et al., 2013. The Mean Composition of Ocean Ridge Basalts. *Geochemistry, Geophysics, Geosystems*, 14(3): 489–518. <https://doi.org/10.1029/2012gc004334>
- Gao, S., Luo, T. C., Zhang, B. R., et al., 1998. Chemical Composition of the Continental Crust as Revealed by Studies in East China. *Geochimica et Cosmochimica Acta*, 62(11): 1959–1975. [https://doi.org/10.1016/s0016-7037\(98\)00121-5](https://doi.org/10.1016/s0016-7037(98)00121-5)
- Glazner, A. F., Farmer, G. L., 1992. Production of Isotopic Variability in Continental Basalts by Cryptic Crustal Contamination. *Science*, 255(5040): 72–74. <https://doi.org/10.1126/science.255.5040.72>
- He, Z. Y., Sun, L. X., Mao, L., et al., 2015. Zircon U-Pb and Hf Isotopic Study of Gneiss and Granodiorite from the Southern Beishan Orogenic Collage: Mesoproterozoic Magmatism and Crustal Growth. *Chinese Science Bulletin*, 60: 389–399. <https://doi.org/10.1360/n972014-00898>
- He, Z. Y., Zhang, Z. M., Zong, K. Q., et al., 2014a. Zircon U-Pb and Hf Isotopic Studies of the Xingxingxia Complex from Eastern Tianshan (NW China): Significance to the Reconstruction and Tectonics of the Southern Central Asian Orogenic Belt. *Lithos*, 190/191: 485–499. <https://doi.org/10.1016/j.lithos.2013.12.023>
- He, Z. Y., Zhang, Z. M., Zong, K. Q., et al., 2014b. Metamorphic *P-T-t* Evolution of Mafic HP Granulites in the Northeastern Segment of the Tarim Craton (Dunhuang Block): Evidence for Early Paleozoic Continental Subduction. *Lithos*, 196/197: 1–13. <https://doi.org/10.1016/j.lithos.2014.02.020>
- Heinonen, J. S., Spera, F. J., Bohrsen, W. A., 2022. Thermodynamic Limits for Assimilation of Silicate Crust in Primitive Magmas. *Geology*, 50(1): 81–85. <https://doi.org/10.1130/g49139.1>
- Hofmann, A. W., 1997. Mantle Geochemistry: The Message from Oceanic Volcanism. *Nature*, 385(6613): 219–229. <https://doi.org/10.1038/385219a0>
- Hofmann, A. W., 2007. Sampling Mantle Heterogeneity through Oceanic Basalts: Isotopes and Trace Elements. *Treatise on Geochemistry*. Elsevier, Amsterdam, 1–44. <https://doi.org/10.1016/b0-08-043751-6/02123-x>
- Hofmann, A. W., Jochum, K. P., Seufert, M., et al., 1986. Nb and Pb in Oceanic Basalts: New Constraints on Mantle Evolution. *Earth and Planetary Science Letters*, 79(1/2): 33–45. [https://doi.org/10.1016/0012-821x\(86\)90038-5](https://doi.org/10.1016/0012-821x(86)90038-5)
- Hu, Z. C., Liu, Y. S., Gao, S., et al., 2012a. A “Wire” Signal Smoothing Device for Laser Ablation Inductively Coupled Plasma Mass Spectrometry Analysis. *Spectrochimica Acta Part B: Atomic Spectroscopy*, 78: 50–57. <https://doi.org/10.1016/j.sab.2012.09.007>
- Hu, Z. C., Gao, S., Liu, Y. S., et al., 2008. Signal Enhancement in Laser Ablation ICP-MS by Addition of Nitrogen in the Central Channel Gas. *Journal of Analytical Atomic Spectrometry*, 23(8): 1093. <https://doi.org/10.1039/b804760j>
- Hu, Z. C., Liu, Y. S., Gao, S., et al., 2012b. Improved *in situ* Hf Isotope Ratio Analysis of Zircon Using Newly Designed X Skimmer Cone and Jet Sample Cone in Combination with the Addition of Nitrogen by Laser Ablation Multiple Collector ICP-MS. *Journal of Analytical Atomic Spectrometry*, 27(9): 1391. <https://doi.org/10.1039/c2ja30078h>
- Jackson, M. G., Hart, S. R., Koppers, A. A. P., et al., 2007. The Return of Subducted Continental Crust in Samoan Lavas. *Nature*, 448(7154): 684–687. <https://doi.org/10.1038/nature06048>
- Jahn, B. M., Wu, F. Y., Hong, D. W., 2000. Important Crustal Growth in the Phanerozoic: Isotopic Evidence of Granitoids from East-Central Asia. *Journal of Earth System Science*, 109(1): 5–20. <https://doi.org/10.1007/bf02719146>
- Jiang, C. Y., Xia, M. Z., Yu, X., et al., 2007. Liuyuan Trachybasalt Belt in the Northeastern Tarim Plate: Products of Asthenosphere Mantle Decompressional Melting. *Acta Petrologica Sinica*, 23(7): 1765–1778 (in Chinese with English Abstract)
- Jung, S., Pfänder, J. A., Brauns, M., et al., 2011. Crustal Contamination and Mantle Source Characteristics in Continental Intra-Plate Volcanic Rocks: Pb, Hf and Os Isotopes from Central European Volcanic Province Basalts. *Geochimica et Cosmochimica Acta*, 75(10): 2664–2683. <https://doi.org/10.1016/j.gca.2011.02.017>
- Kröner, A., 2007. Chapter 5.2 the Ancient Gneiss Complex of Swaziland and Environs: Record of Early Archean Crustal Evolution in Southern Africa. *Developments in Precambrian Geology*, 15: 465–480. [https://doi.org/10.1016/s0166-2635\(07\)15052-0](https://doi.org/10.1016/s0166-2635(07)15052-0)
- Lee, C. T., 2014. Physics and Chemistry of Deep Continental Crust Recycling. *Treatise on Geochemistry (Second Edition)*, 4: 423–456. <https://doi.org/10.1016/b978-0-08-095975-7.00314-4>
- Li, J., Wu, C., Chen, X. H., et al., 2022. Tectonic Evolution of the Beishan Orogen in Central Asia: Subduction, Accretion, and Continent-Continent Collision during the Closure of the Paleo-Asian Ocean. *GSA Bulletin*, online. <https://doi.org/10.1130/b36451.1>
- Liu, S. N., Zhou, L. Y., Wang, Y., 2022. Missing Adakitic Granite and Syn-Subduction Mafic Dikes within Permian Volcanic Belts of the Southern Margin of the CAO? Comment on “Permian Oceanic Slab Subduction in the Southernmost Central Asian Orogenic Belt: Evidence from Adakite and High-Mg Diorite in the Southern Beishan”. *Lithos*, 412/413: 106025. <https://doi.org/10.1016/j.lithos.2021.106025>
- Liu, X. C., Chen, B. L., Jahn, B. M., et al., 2011. Early Paleozoic (Ca. 465 Ma) Eclogites from Beishan (NW China) and Their Bearing on the Tectonic Evolution of the Southern Central Asian Orogenic Belt. *Journal of Asian Earth Sciences*, 42(4): 715–731. <https://doi.org/10.1016/j.jseas.2011.02.001>

- 10.1016/j.jseae.2010.10.017
- Liu, Y. S., Gao, S., Hu, Z. C., et al., 2010. Continental and Oceanic Crust Recycling-Induced Melt-Peridotite Interactions in the Trans-North China Orogen: U-Pb Dating, Hf Isotopes and Trace Elements in Zircons from Mantle Xenoliths. *Journal of Petrology*, 51(1/2): 537–571. <https://doi.org/10.1093/ptrology/egp082>
- Liu, Y. S., Hu, Z. C., Gao, S., et al., 2008a. *In situ* Analysis of Major and Trace Elements of Anhydrous Minerals by LA-ICP-MS without Applying an Internal Standard. *Chemical Geology*, 257(1/2): 34–43. <https://doi.org/10.1016/j.chemgeo.2008.08.004>
- Liu, Y. S., Zong, K. Q., Kelemen, P. B., et al., 2008b. Geochemistry and Magmatic History of Eclogites and Ultramafic Rocks from the Chinese Continental Scientific Drill Hole: Subduction and Ultrahigh-Pressure Metamorphism of Lower Crustal Cumulates. *Chemical Geology*, 247(1/2): 133–153. <https://doi.org/10.1016/j.chemgeo.2007.10.016>
- Ludwig, K. R., 2003. Isoplot 3.00: A Geochronological Toolkit for Microsoft Excel. *Berkeley Geochronology Center Special Publication*, 4: 70
- Ma, Q., Zheng, J. P., Griffin, W. L., et al., 2012. Triassic “Adakitic” Rocks in an Extensional Setting (North China): Melts from the Cratonic Lower Crust. *Lithos*, 149: 159–173. <https://doi.org/10.1016/j.lithos.2012.04.017>
- Mantle, G. W., Collins, W. J., 2008. Quantifying Crustal Thickness Variations in Evolving Orogens: Correlation between Arc Basalt Composition and Moho Depth. *Geology*, 36(1): 87–90. <https://doi.org/10.1130/g24095a.1>
- Mao, Q. G., Xiao, W. J., Windley, B. F., et al., 2012. The Liuyuan Complex in the Beishan, NW China: A Carboniferous–Permian Ophiolitic Fore-Arc Sliver in the Southern Altaids. *Geological Magazine*, 149(3): 483–506. <https://doi.org/10.1017/s0016756811000811>
- McBride, J. S., Lambert, D. D., Nicholls, I. A., et al., 2001. Osmium Isotopic Evidence for Crust-Mantle Interaction in the Genesis of Continental Intraplate Basalts from the Newer Volcanics Province, Southeastern Australia. *Journal of Petrology*, 42(6): 1197–1218. <https://doi.org/10.1093/ptrology/42.6.1197>
- McDonough, W. F., Sun, S. S., 1995. The Composition of the Earth. *Chemical Geology*, 120(3/4): 223–253. [https://doi.org/10.1016/0009-2541\(94\)00140-4](https://doi.org/10.1016/0009-2541(94)00140-4)
- O’Hara, M. J., Herzberg, C., 2002. Interpretation of Trace Element and Isotope Features of Basalts: Relevance of Field Relations, Petrology, Major Element Data, Phase Equilibria, and Magma Chamber Modeling in Basalt Petrogenesis. *Geochimica et Cosmochimica Acta*, 66(12): 2167–2191. [https://doi.org/10.1016/s0016-7037\(02\)00852-9](https://doi.org/10.1016/s0016-7037(02)00852-9)
- Pearce, J. A., 2008. Geochemical Fingerprinting of Oceanic Basalts with Applications to Ophiolite Classification and the Search for Archean Oceanic Crust. *Lithos*, 100(1/2/3/4): 14–48. <https://doi.org/10.1016/j.lithos.2007.06.016>
- Pearce, J. A., 2003. Supra-Subduction Zone Ophiolites: The Search for Modern Analogues. *Special Paper of the Geological Society of America*, 373: 269–293
- Pearce, J. A., Peate, D. W., 1995. Tectonic Implications of the Composition of Volcanic ARC Magmas. *Annual Review of Earth and Planetary Sciences*, 23: 251–285. <https://doi.org/10.1146/annurev.ea.23.050195.001343>
- Qin, K. Z., Su, B. X., Sakyi, P. A., et al., 2011. SIMS Zircon U-Pb Geochronology and Sr-Nd Isotopes of Ni-Cu-Bearing Mafic-Ultramafic Intrusions in Eastern Tianshan and Beishan in Correlation with Flood Basalts in Tarim Basin (NW China): Constraints on a ca. 280 Ma Mantle Plume. *American Journal of Science*, 311(3): 237–260. <https://doi.org/10.2475/03.2011.03>
- Qu, J. F., Xiao, W. J., Windley, B. F., et al., 2011. Ordovician Eclogites from the Chinese Beishan: Implications for the Tectonic Evolution of the Southern Altaids. *Journal of Metamorphic Geology*, 29(8): 803–820. <https://doi.org/10.1111/j.1525-1314.2011.00942.x>
- Reiners, P. W., Nelson, B. K., Ghiorsio, M. S., 1995. Assimilation of Felsic Crust by Basaltic Magma: Thermal Limits and Extents of Crustal Contamination of Mantle-Derived Magmas. *Geology*, 23(6): 563. [https://doi.org/10.1130/0091-7613\(1995\)0230563:aofcbb>2.3.co;2](https://doi.org/10.1130/0091-7613(1995)0230563:aofcbb>2.3.co;2)
- Rudnick, R., Gao, S., 2003. Composition of the Continental Crust. *Treatise on Geochemistry*, 3: 1–64. <https://doi.org/10.1016/b0-08-043751-6/03016-4>
- Rudnick, R. L., Fountain, D. M., 1995. Nature and Composition of the Continental Crust: A Lower Crustal Perspective. *Reviews of Geophysics*, 33(3): 267–309. <https://doi.org/10.1029/95rg01302>
- Saktura, W. M., Buckman, S., Nutman, A. P., et al., 2017. Continental Origin of the Gubaoquan Eclogite and Implications for Evolution of the Beishan Orogen, Central Asian Orogenic Belt, NW China. *Lithos*, 294/295: 20–38. <https://doi.org/10.1016/j.lithos.2017.10.004>
- Song, D. F., Xiao, W. J., Han, C. M., et al., 2013. Progressive Accretionary Tectonics of the Beishan Orogenic Collage, Southern Altaids: Insights from Zircon U-Pb and Hf Isotopic Data of High-Grade Complexes. *Precambrian Research*, 227: 368–388. <https://doi.org/10.1016/j.precamres.2012.06.011>
- Song, D. F., Xiao, W. J., Windley, B. F., et al., 2015. A Paleozoic Japan-Type Subduction-Accretion System in the Beishan Orogenic Collage, Southern Central Asian Orogenic Belt. *Lithos*, 224/225: 195–213. <https://doi.org/10.1016/j.lithos.2015.03.005>
- Su, B. X., Qin, K. Z., Santosh, M., et al., 2013. The Early Permian Mafic-Ultramafic Complexes in the Beishan Terrane, NW China: Alaskan-Type Intrusives or Rift Cumulates? *Journal of Asian Earth Sciences*, 66: 175–187. <https://doi.org/10.1016/j.jseae.2012.12.039>
- Su, B. X., Qin, K. Z., Sun, H., et al., 2012. Subduction-Induced Mantle Heterogeneity beneath Eastern Tianshan and Beishan: Insights from Nd-Sr-Hf-O Isotopic Mapping of Late Paleozoic Mafic-Ultramafic Complexes. *Lithos*, 134/135: 41–51. <https://doi.org/10.1016/j.lithos.2011.12.011>
- Wang, Q., Wyman, D. A., Zhao, Z. H., et al., 2007. Petrogenesis of Carboniferous Adakites and Nb-Enriched Arc Basalts in the Alataw Area, Northern Tianshan Range (Western China): Implications for Phanerozoic Crustal Growth in the Central Asia Orogenic Belt. *Chemical Geology*, 236(1/2): 42–64. <https://doi.org/10.1016/j.chemgeo.2006.08.013>
- Wang, S. J., Li, S. C., Li, W. J., et al., 2020. Tectonic Evolution of Southeast Central Asian Orogenic Belt: Evidence from Geochronological Data and Paleontology of the Early Paleozoic Deposits in Inner Mongolia. *Journal of Earth Science*, 31(4): 743–756. <https://doi.org/10.1007/s12583-020-1326-6>
- Wang, T., Huang, H., Song, P., et al., 2020. Studies of Crustal Growth and Deep Lithospheric Architecture and New Issues: Exemplified by the Central Asian Orogenic Belt (Northern Xinjiang). *Earth Science*, 45(7): 2326–2344 (in Chinese with English Abstract)
- Wang, Y., Luo, Z. H., Santosh, M., et al., 2017. The Liuyuan Volcanic Belt in NW China Revisited: Evidence for Permian Rifting Associated with the Assembly of Continental Blocks in the Central Asian Orogenic Belt. *Geological Magazine*, 154(2): 265–285. <https://doi.org/10.1017/s0016756815001077>
- White, W. M., 2010. Oceanic Island Basalts and Mantle Plumes: The Geochemical Perspective. *Annual Review of Earth and Planetary Sciences*, 38: 133–160. <https://doi.org/10.1146/annurev-earth-040809->

- 152450
- White, W. M., 2015. Isotopes, DUPAL, LLSVPS, and Anekantavada. *Chemical Geology*, 419: 10–28. <https://doi.org/10.1016/j.chemgeo.2015.09.026>
- White, W. M., Hofmann, A. W., 1982. Sr and Nd Isotope Geochemistry of Oceanic Basalts and Mantle Evolution. *Nature*, 296(5860): 821–825. <https://doi.org/10.1038/296821a0>
- Windley, B. F., Alexeiev, D., Xiao, W. J., et al., 2007. Tectonic Models for Accretion of the Central Asian Orogenic Belt. *Journal of the Geological Society*, 164(1): 31–47. <https://doi.org/10.1144/0016-76492006-022>
- Workman, R. K., Hart, S. R., 2005. Major and Trace Element Composition of the Depleted MORB Mantle (DMM). *Earth and Planetary Science Letters*, 231(1/2): 53–72. <https://doi.org/10.1016/j.epsl.2004.12.005>
- Workman, R. K., Hart, S. R., Jackson, M., et al., 2004. Recycled Metasomatized Lithosphere as the Origin of the Enriched Mantle II (EM2) End-Member: Evidence from the Samoan Volcanic Chain. *Geochemistry, Geophysics, Geosystems*, 5(4): Q04008. <https://doi.org/10.1029/2003gc000623>
- Wu, C., Yin, A., Zuza, A. V., et al., 2016. Pre-Cenozoic Geologic History of the Central and Northern Tibetan Plateau and the Role of Wilson Cycles in Constructing the Tethyan Orogenic System. *Lithosphere*, 8(3): 254–292. <https://doi.org/10.1130/L494.1>
- Xiao, W. J., Mao, Q. G., Windley, B. F., et al., 2010. Paleozoic Multiple Accretionary and Collisional Processes of the Beishan Orogenic Collage. *American Journal of Science*, 310(10): 1553–1594. <https://doi.org/10.2475/10.2010.12>
- Xiao, W. J., Windley, B. F., Han, C. M., et al., 2018. Late Paleozoic to Early Triassic Multiple Roll-Back and Oroclinal Bending of the Mongolia Collage in Central Asia. *Earth-Science Reviews*, 186: 94–128. <https://doi.org/10.1016/j.earscirev.2017.09.020>
- Xiao, W. J., Windley, B. F., Huang, B. C., et al., 2009. End-Permian to Mid-Triassic Termination of the Accretionary Processes of the Southern Altaids: Implications for the Geodynamic Evolution, Phanerozoic Continental Growth, and Metallogeny of Central Asia. *International Journal of Earth Sciences*, 98(6): 1189–1217. <https://doi.org/10.1007/s00531-008-0407-z>
- Xiao, W. J., Windley, B. F., Sun, S., et al., 2015. A Tale of Amalgamation of Three Permo-Triassic Collage Systems in Central Asia: Oroclines, Sutures, and Terminal Accretion. *Annual Review of Earth and Planetary Sciences*, 43: 477–507. <https://doi.org/10.1146/annurev-earth-060614-105254>
- Xu, W., Xu, X. Y., Niu, Y. Z., et al., 2019. Geochronology and Petrogenesis of the Permian Marine Basalt in the Southern Beishan Region and Their Tectonic Implications. *Acta Geologica Sinica*, 93(8): 1928–1953. <https://doi.org/10.19762/j.cnki.dizhixuebao.2019167>
- Xu, W., Xu, X. Y., Niu, Y. Z., et al., 2018. Geochronology, Petrogenesis and Tectonic Implications of Early Permian A-Type Rhyolite from Southern Beishan Orogen, NW China. *Acta Petrologica Sinica*, 34(10): 3011–3033. [https://doi.org/1000-0569/2018/034\(10\)-3011-33](https://doi.org/1000-0569/2018/034(10)-3011-33)
- Xue, S. C., Li, C. S., Qin, K. Z., et al., 2016. A Non-Plume Model for the Permian Protracted (266–286 Ma) Basaltic Magmatism in the Beishan-Tianshan Region, Xinjiang, Western China. *Lithos*, 256/257: 243–249. <https://doi.org/10.1016/j.lithos.2016.04.018>
- Yuan, Y., Zong, K. Q., Cawood, P. A., et al., 2019. Implication of Mesoproterozoic (~1.4 Ga) Magmatism within Microcontinents along the Southern Central Asian Orogenic Belt. *Precambrian Research*, 327: 314–326. <https://doi.org/10.1016/j.precamres.2019.03.014>
- Yuan, Y., Zong, K. Q., He, Z. Y., et al., 2015. Geochemical and Geochronological Evidence for a Former Early Neoproterozoic Microcontinent in the South Beishan Orogenic Belt, Southernmost Central Asian Orogenic Belt. *Precambrian Research*, 266: 409–424. <https://doi.org/10.1016/j.precamres.2015.05.034>
- Zeng, G., Chen, L. H., Hofmann, A. W., et al., 2011. Crust Recycling in the Sources of Two Parallel Volcanic Chains in Shandong, North China. *Earth and Planetary Science Letters*, 302(3/4): 359–368. <https://doi.org/10.1016/j.epsl.2010.12.026>
- Zhang, W., Hu, Z. C., 2020. Estimation of Isotopic Reference Values for Pure Materials and Geological Reference Materials. *Atomic Spectroscopy*, 41(3): 93–102. <https://doi.org/10.46770/as.2020.03.001>
- Zhang, W., Hu, Z. C., Liu, Y. S., 2020. Iso-Compass: New Freeware Software for Isotopic Data Reduction of LA-MC-ICP-MS. *Journal of Analytical Atomic Spectrometry*, 35(6): 1087–1096. <https://doi.org/10.1039/d0ja00084a>
- Zhang, W., Pease, V., Wu, T. R., et al., 2012a. Discovery of an Adakite-Like Pluton near Dongqiyishan (Beishan, NW China)—Its Age and Tectonic Significance. *Lithos*, 142/143: 148–160. <https://doi.org/10.1016/j.lithos.2012.02.021>
- Zhang, W., Wu, T. R., Zheng, R. G., et al., 2012b. Post-Collisional Southeastern Beishan Granites: Geochemistry, Geochronology, Sr-Nd-Hf Isotopes and Their Implications for Tectonic Evolution. *Journal of Asian Earth Sciences*, 58: 51–63. <https://doi.org/10.1016/j.jseae.2012.07.004>
- Zhang, Y. Y., Dostal, J., Zhao, Z. H., et al., 2011. Geochronology, Geochemistry and Petrogenesis of Mafic and Ultramafic Rocks from Southern Beishan Area, NW China: Implications for Crust-Mantle Interaction. *Gondwana Research*, 20(4): 816–830. <https://doi.org/10.1016/j.gr.2011.03.008>
- Zhang, Y. Y., Yuan, C., Sun, M., et al., 2017. Arc Magmatism Associated with Steep Subduction: Insights from Trace Element and Sr-Nd-Hf-B Isotope Systematics. *Journal of Geophysical Research: Solid Earth*, 122(3): 1816–1834. <https://doi.org/10.1002/2016jb013289>
- Zhang, Y. Y., Yuan, C., Sun, M., et al., 2015. Permian Doleritic Dikes in the Beishan Orogenic Belt, NW China: Asthenosphere-Lithosphere Interaction in Response to Slab Break-off. *Lithos*, 233: 174–192. <https://doi.org/10.1016/j.lithos.2015.04.001>
- Zhao, Z. H., Guo, Z. J., Han, B. F., et al., 2006. Comparative Study on Permian Basalts from Eastern Xinjiang-Beishan Area of Gansu Province and Its Tectonic Implications. *Acta Petrologica Sinica*, 22(5): 1279–1293 (in Chinese with English Abstract)
- Zheng, R. G., Li, J. Y., Zhang, J., et al., 2020. Permian Oceanic Slab Subduction in the Southmost of Central Asian Orogenic Belt: Evidence from Adakite and High-Mg Diorite in the Southern Beishan. *Lithos*, 358/359: 105406. <https://doi.org/10.1016/j.lithos.2020.105406>
- Zheng, R. G., Wu, T. R., Zhang, W., et al., 2014. Geochronology and Geochemistry of Late Paleozoic Magmatic Rocks in the Yinwaxia Area, Beishan: Implications for Rift Magmatism in the Southern Central Asian Orogenic Belt. *Journal of Asian Earth Sciences*, 91: 39–55. <https://doi.org/10.1016/j.jseae.2014.04.022>
- Zhou, M. F., Leshner, C. M., Yang, Z. X., et al., 2004. Geochemistry and Petrogenesis of 270 Ma Ni-Cu-(PGE) Sulfide-Bearing Mafic Intrusions in the Huangshan District, Eastern Xinjiang, Northwest China: Implications for the Tectonic Evolution of the Central Asian Orogenic Belt. *Chemical Geology*, 209(3/4): 233–257. <https://doi.org/10.1016/j.chemgeo.2004.05.005>
- Zindler, A., Hart, S., 1986. Chemical Geodynamics. *Annual Review of Earth*

- and Planetary Sciences*, 14: 493–571. <https://doi.org/10.1146/annurev.ea.14.050186.002425>
- Zong, K. Q., Zhang, Z. M., He, Z. Y., et al., 2012. Early Palaeozoic High-Pressure Granulites from the Dunhuang Block, Northeastern Tarim Craton: Constraints on Continental Collision in the Southern Central Asian Orogenic Belt. *Journal of Metamorphic Geology*, 30(8): 753–768. <https://doi.org/10.1111/j.1525-1314.2012.00997.x>
- Zuo, G. C., Zhang, S. L., He, G. Q., et al., 1991. Plate Tectonic Characteristics during the Early Paleozoic in Beishan near the Sino-Mongolian Border Region, China. *Tectonophysics*, 188(3/4): 385–392. [https://doi.org/10.1016/0040-1951\(91\)90466-6](https://doi.org/10.1016/0040-1951(91)90466-6)